Aire-dependent production of XCL1 mediates medullary accumulation of thymic dendritic cells and contributes to regulatory T cell development

Yu Lei,[1,3] Adiratna Mat Ripen,[1] Naozumi Ishimaru,[2] Izumi Ohigashi,[1] Takashi Nagasawa,[4] Lukas T. Jeker,[5] Michael R. Bösl,[6] Georg A. Holländer,[5] Yoshio Hayashi,[2] Rene de Waal Malefyt,[7] Takeshi Nitta,[1] and Yousuke Takahama[1]

[1]Division of Experimental Immunology, Institute for Genome Research, [2]Department of Oral Molecular Pathology, Institute of Health Biosciences, University of Tokushima, Tokushima 770-8503, Japan
[3]Key Laboratory of Molecular Biology for Infectious Disease of the People's Republic of China Ministry of Education, Institute for Viral Hepatitis, The Second Affiliated Hospital, Chongqing Medical University, Chongqing 400010, China
[4]Department of Immunobiology and Hematology, Institute for Frontier Medical Sciences, Kyoto University, Kyoto 606-8507, Japan
[5]Laboratory of Pediatric Immunology, Center for Biomedicine, University of Basel and The University Children's Hospital of Basel, 4058 Basel, Switzerland
[6]Transgenic Core Facility, Max-Planck-Institute of Biochemistry, 82152 Martinsried, Germany
[7]Merck Research Laboratories, Palo Alto, CA 94304

Dendritic cells (DCs) in the thymus (tDCs) are predominantly accumulated in the medulla and contribute to the establishment of self-tolerance. However, how the medullary accumulation of tDCs is regulated and involved in self-tolerance is unclear. We show that the chemokine receptor XCR1 is expressed by tDCs, whereas medullary thymic epithelial cells (mTECs) express the ligand XCL1. XCL1-deficient mice are defective in the medullary accumulation of tDCs and the thymic generation of naturally occurring regulatory T cells (nT reg cells). Thymocytes from XCL1-deficient mice elicit dacryoadenitis in *nude* mice. mTEC expression of XCL1, tDC medullary accumulation, and nT reg cell generation are diminished in Aire-deficient mice. These results indicate that the XCL1-mediated medullary accumulation of tDCs contributes to nT reg cell development and is regulated by Aire.

CORRESPONDENCE
Yousuke Takahama:
takahama@
genome.tokushima-u.ac.jp

Abbreviations used: cTEC, cortical thymic epithelial cell; CMJ, cortico-medullary junction; mOVA, membrane-bound OVA; mTEC, medullary thymic epithelial cell; *Mtv*, *mammary tumor virus*; nT reg cell, naturally occurring regulatory T cell; RIP, rat insulin promoter; SCZ, subcapsular zone; tDC, thymic DC.

The thymus provides a microenvironment that is central to the establishment of self-tolerance (Takahama, 2006; Anderson et al., 2007; Klein et al., 2009). In the medullary region of the thymus, medullary thymic epithelial cells (mTECs) and thymic DCs (tDCs) display systemic and tissue-restricted self-antigens and cooperate to induce the negative selection of self-reactive thymocytes (Liston et al., 2003; Gallegos and Bevan, 2004; Anderson et al., 2005). mTECs express a diverse set of self-antigens, including the promiscuously expressed tissue-restricted antigens, in part regulated by the nuclear protein Aire (Derbinski et al., 2001; Anderson et al., 2002). tDCs cross-present the mTEC-derived self-antigens (Gallegos and Bevan, 2004), whereas a fraction of tDCs are derived from the circulation importing various self-antigens into the thymus (Bonasio et al., 2006). The cooperation between mTECs and tDCs contributes to the negative selection of tissue-restricted antigen-reactive thymocytes (Gallegos and Bevan, 2004). In addition to the negative selection of self-reactive thymocytes, the thymus produces naturally occurring regulatory T cells (nT reg cells) that are essential for the establishment of self-tolerance (Sakaguchi et al., 2008). It has been suggested that mTECs (Aschenbrenner et al., 2007; Spence and Green, 2008), tDCs (Proietto et al., 2008; Hanabuchi et al., 2010), and their cooperation (Watanabe et al., 2005)

The Rockefeller University Press $30.00
J. Exp. Med. Vol. 208 No. 2 383-394
www.jem.org/cgi/doi/10.1084/jem.20102327

The Journal of Experimental Medicine

contribute to the generation of nT reg cells in the thymus. However, how these cells contribute to and/or cooperate for the generation of nT reg cells is still elusive.

tDCs are predominantly accumulated in the medullary region of the thymus and sparsely detectable in the cortex (Barclay and Mayrhofer, 1981; Flotte et al., 1983; Kurobe et al., 2006). The accumulation of tDCs in the medulla is presumed to contribute to their efficient cooperation with mTECs in the establishment of negative selection and nT reg cell generation. Nonetheless, how tDCs are accumulated in the thymic medulla and how this medullary accumulation of tDCs contributes to negative selection and nT reg cell generation are unknown. The present study identifies the chemokine XCL1, also known as lymphotactin, as being essential for the medullary accumulation of tDCs. Cells that produce XCL1 in the thymus include mTECs, whereas XCR1, the receptor for XCL1, is expressed by tDCs. We also find that Aire is essential for the mTEC production of XCL1. In mice deficient for XCL1 or Aire, most tDCs fail to accumulate in the medulla and are arrested at the cortico-medullary junction (CMJ). The generation of nT reg cells is impaired in both *Xcl1*-deficient mice and *Aire*-deficient mice. Like *Aire*-deficient mice (Anderson et al., 2002, 2005), *nude* mice transferred with thymocytes from *Xcl1*-deficient mice exhibit inflammatory lesions in lacrimal glands. These results reveal that the XCL1-mediated medullary accumulation of tDCs critically contributes to the development of nT reg cells, and they suggest a role for Aire in facilitating the XCL1-mediated medullary accumulation of tDCs.

RESULTS

Screening for chemokines involved in the localization of tDCs

tDCs are predominantly accumulated in the medulla and sparsely detectable in the cortex (Barclay and Mayrhofer, 1981; Flotte et al., 1983; Kurobe et al., 2006). To identify chemokines that mediate the medullary accumulation of tDCs, we screened for the expression of chemokine receptors in isolated tDCs by RT-PCR analysis. Among the mouse chemokine receptors so far identified, *Ccr2*, *Ccr4*, *Ccr5*, *Ccr6*, *Ccr7*, *Ccr8*, *Cxcr1*, *Cxcr3*, *Cxcr4*, *Xcr1*, and *Cx3cr1* were detected in CD11c$^+$ cells isolated from the thymus (Fig. 1 A). We then examined chemokines that could bind to these transcript-detectable receptors for their ability to attract CD11c$^+$ thymic cells. We found that CCL19 (CCR7 ligand), CCL21 (CCR7 ligand), CXCL12 (CXCR4 ligand), or XCL1 (XCR1 ligand) attracted CD11c$^+$ thymic cells (Fig. 1 B). These results revealed the potential roles of CCR7, CXCR4, and XCR1 in the chemotactic regulation of tDCs. However, we detected no obvious defects in the medullary accumulation of CD11c$^+$ DCs in the thymus of mice deficient for CCR7, CCR7 ligands, or CXCR4 (Fig. 1 C; also see Fig. 3 D), even though the medullary region in CCR7- or CCR7 ligand–deficient mice was smaller than that in control mice (Fig. 1 C; Kurobe et al., 2006; Nitta et al., 2009). Thus, instead of CCR7 and CXCR4, the XCL1–XCR1 chemokine axis may play a major role in regulating the medullary accumulation of tDCs.

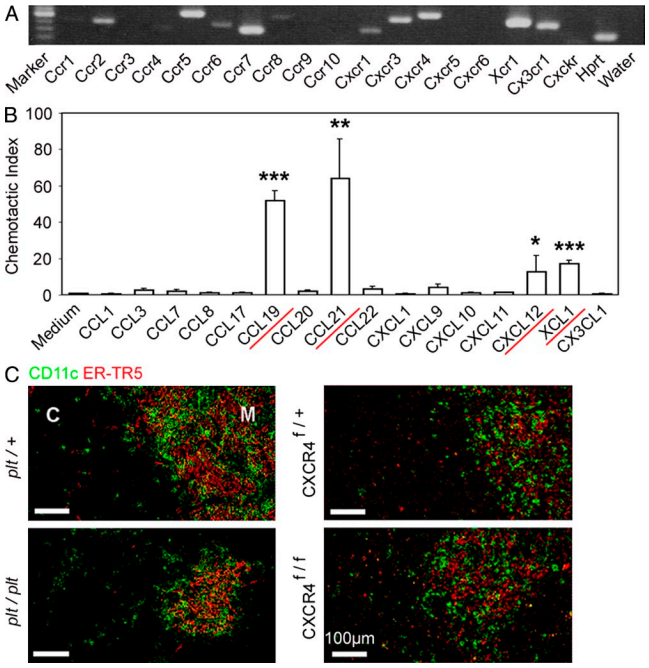

Figure 1. Screening for chemokines that regulate the localization of tDCs. (A) RT-PCR analysis of chemokine receptor expression in isolated tDCs. Shown are the results of ethidium bromide detection of electrophoretically separated PCR products. Hprt, hypoxanthine-guanine phosphoribosyltransferase. Shown are the representative data of three independent experiments. (B) Chemotactic indexes of tDCs to the ligands of expressed chemokine receptors CCL1 (CCR8 ligand), CCL3 (CCR5 ligand), CCL7 (CCR2 ligand), CCL8 (CCR5 ligand), CCL17 (CCR4 ligand), CCL19 (CCR7 ligand), CCL20 (CCR6 ligand), CCL21 (CCR7 ligand), CCL22 (CCR4 ligand), CXCL1 (CXCR1 ligand), CXCL9 (CXCR3 ligand), CXCL10 (CXCR3 ligand), CXCL11 (CXCR3 ligand), CXCL12 (CXCR4 ligand), XCL1 (XCR1 ligand), and CX3CL1 (CX3CR1 ligand) were determined. Bar graphs indicate means ± standard errors of the data from at least three independent measurements. Red underlines indicate the chemokines that attracted the tDCs (based on the statistical significance as shown in the graph). *, $P < 0.05$; **, $P < 0.01$; ***, $P < 0.001$. (C) Frozen thymus sections from CCR7 ligand–deficient (*plt/plt*) and CXCR4-deficient (Mx-Cre x CXCR4$^{f/f}$) mice, as well as the control mice, were stained with anti-CD11c antibody (green) and mTEC-specific antibody ER-TR5 (red). The majority, if not all, of *Cxcr4* was deleted in the thymus cells of Mx-Cre x CXCR4$^{f/f}$ mice. C, cortex; M, medulla. Shown are the representative results of three independent experiments.

Xcr1 expression by tDCs and *Xcl1* expression by mTECs

We next examined the expression of *Xcr1* and *Xcl1* in various cell populations in the thymus. We found that *Xcr1* transcripts in the thymus were detected exclusively in CD11c$^+$ tDCs and not in CD45$^+$ total thymocytes, CD11b$^+$CD11c$^-$ macrophages, or nonhematopoietic thymic stromal cells, including CD45$^-$I-A$^+$UEA1$^+$ mTECs and CD45$^-$I-A$^+$Ly51$^+$ cortical thymic epithelial cells (cTECs; Fig. 2 A). Among tDCs, *Xcr1* was most highly expressed in I-A^{high}CD11c^{high}CD11b$^-$ lymphoid DCs compared with I-A^{high}CD11c^{high}CD11b$^+$ myeloid DCs or I-A^{medium}CD11c^{medium}B220$^+$ plasmacytoid DCs (Fig. 2 B). Comparable amounts of *Xcr1* were detected in DCs from the thymus, spleen, subcutaneous lymph nodes,

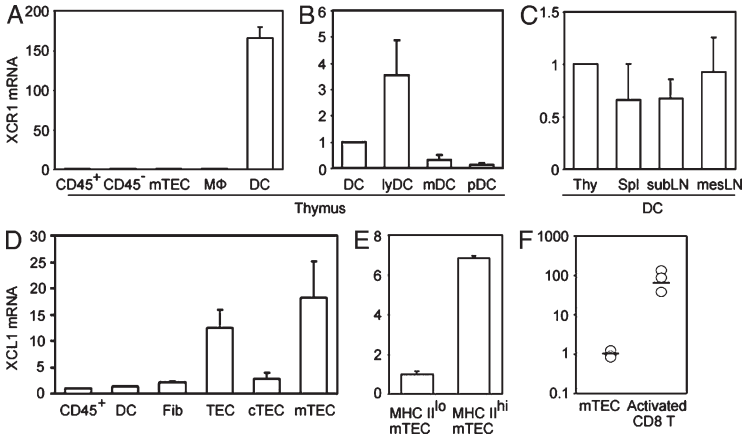

Figure 2. Expression of *Xcr1* and *Xcl1* in the thymus. (A–C) Quantitative RT-PCR analysis of *Xcr1* expression in sorted thymus cell populations, including CD45$^+$ thymocytes (CD45$^+$), CD45$^-$ thymic stromal cells (CD45$^-$), CD45$^-$I-A$^+$UEA1$^+$ mTECs, CD11b$^+$CD11c$^-$ macrophages (MΦ), and CD11c$^+$ tDCs (A); in sorted tDC subpopulations, including CD11c$^+$ total tDCs, I-A^{high}CD11c^{high}CD11b$^-$ lymphoid tDCs (lyDC), I-A^{high}CD11c^{high}CD11b$^+$ myeloid tDCs (mDC), and I-A^{medium}CD11c^{medium}B220$^+$ plasmacytoid tDCs (pDC) (B); and in CD11c$^+$ DCs from the thymus (Thy), the spleen (Spl), the subcutaneous lymph nodes (subLN), and the mesenteric lymph nodes (mesLN; C). The amounts of *Xcr1* were normalized to the amount of *Hprt*, and those in CD45$^+$ thymocytes (A) and total tDCs (B and C) were arbitrarily set to 1. (D and E) Quantitative RT-PCR analysis of *Xcl1* expression in thymus cell populations, including CD45$^+$ thymocytes (CD45$^+$), CD11c$^+$ DCs, CD45$^-$I-A$^-$MTS15$^+$ fibroblasts (Fib), CD45$^-$I-A$^+$ total TECs (TEC), CD45$^-$I-A$^+$Ly51$^+$ cTECs (cTEC), and CD45$^-$I-A$^+$UEA1$^+$ mTECs (mTEC); and in CD45$^-$I-A^{low}UEA1$^+$ (MHC II^{lo}) and CD45$^-$I-A^{high}UEA1$^+$ (MHC II^{hi}) mTEC subpopulations. The amounts of *Xcl1* were normalized to the amount of *Hprt*, and those in CD45$^+$ thymocytes (D) and CD45$^-$ I-A^{low}UEA1$^+$ mTECs (E) were arbitrarily set to 1. Bar graphs show means and standard errors of at least three independent measurements. (F) Quantitative RT-PCR analysis of *Xcl1* expression in CD45$^-$I-A$^+$UEA1$^+$ mTECs and anti-CD3–stimulated CD8$^+$ T cells. Means (bars) and individual measurements (circles) are shown (n = 3).

and mesenteric lymph nodes (Fig. 2 C). In contrast, *Xcl1* transcripts in the thymus were detected in CD45$^-$I-A$^+$UEA1$^+$ mTECs rather than CD45$^+$ thymocytes, CD11c$^+$ tDCs, CD45$^-$I-A$^-$MTS15$^+$ fibroblasts, or CD45$^-$I-A$^+$Ly51$^+$ cTECs (Fig. 2 D). Among the mTECs, *Xcl1* was prominently detected in CD45$^-$I-A^{high}UEA1$^+$ (MHC II^{hi}) mTECs rather than CD45$^-$I-A^{low}UEA1$^+$ (MHC II^{lo}) mTECs (Fig. 2 E). In addition to mTECs, *Xcl1* was also detected in a small subpopulation of CD45$^+$ thymocytes expressing NK1.1, including NK1.1$^+$CD3$^-$ NK cells and NK1.1$^+$CD3$^+$ NKT cells (Kelner et al., 1994; Hedrick et al., 1997; unpublished data). Previous studies showed that *Xcl1* is expressed in the secondary lymphoid organs by Th1-polarized CD4$^+$ T cells and activated CD8$^+$ T cells (Dorner et al., 2002, 2009). The expression of *Xcl1* in mTECs was lower than that in activated CD8$^+$ T cells (Fig. 2 F). However, in the thymus, XCL1 is prominently produced by a fraction of mTECs, whereas its receptor XCR1 is exclusively expressed by tDCs.

Role of *Xcl1* in medullary accumulation of tDCs

To examine whether XCL1 plays a role in the localization of tDCs, we generated *Xcl1*-deficient mice (Fig. S1). In the thymus of *Xcl1*-deficient mice, we found that the medullary region was not densely populated with CD11c$^+$ tDCs (Fig. 3 A). Measurement of tDC density in various regions of the thymus sections (Fig. S2 A) indicated that the number of tDCs per unit area in the middle medullary region (M region) was significantly ($P < 0.001$) decreased in *Xcl1*-deficient mice as compared with control mice, whereas the number of tDCs per unit area in the deep cortical region close to the CMJ (CMJ-C region) was significantly ($P < 0.01$) elevated in *Xcl1*-deficient mice as compared with control mice (Fig. 3, A and B). In contrast, the densities of tDCs in the subcapsular zone (SCZ) region, the middle cortical region (C region), and the peripheral medullary region close to the CMJ (CMJ-M region) were not significantly ($P > 0.05$) altered by the *Xcl1* deficiency (Fig. 3, A and B). Similarly to *Xcl1*-deficient mice of BALB/c background, *Xcl1*-deficient mice of C57BL/6 background exhibited altered distribution of tDCs, namely sparseness in the M region and density in the CMJ-C region (Fig. S2 B). Nonetheless, the absolute numbers of tDCs, including lymphoid DC, myeloid DC, and plasmacytoid DC subsets, were not affected in *Xcl1*-deficient mice (Fig. 3 C). These results indicate that XCL1 is essential for the accumulation of tDCs in the inner medullary region and that the deficiency of XCL1 causes the aberrant arrest of tDCs in the CMJ-C region.

The localization of tDCs was specifically altered in *Xcl1*-deficient mice but not in CCR7 ligand–deficient *plt/plt* mice or CXCR4-deficient mice (Fig. 1 C and Fig. 3 D). The defective accumulation of tDCs in the thymic medulla caused by the XCL1 deficiency was not further compromised by an additional lack of CCR7 ligands (Fig. 3 D). Thus, among the chemokines that exert chemotactic activity on tDCs (Fig. 1 B), XCL1 appears to be the major regulator of the tDC medullary accumulation.

Unlike tDCs, CD11b$^+$ macrophages in the thymus were not enriched in the medulla of WT mice but were most densely distributed in the CMJ-C region (Fig. 3, E and F). This distribution was not affected in *Xcl1*-deficient mice (Fig. 3, E and F). The distribution and number of CD4$^+$CD8$^+$, CD4$^+$CD8$^-$, or CD4$^-$CD8$^+$ thymocytes were normal in *Xcl1*-deficient mice (unpublished data). These results indicate that in the thymus, XCL1 influences the distribution of tDCs specifically.

Negative selection of self-reactive thymocytes in *Xcl1*-deficient mice

It was previously shown that tDCs contribute to the negative selection of self-reactive thymocytes (Jenkinson et al., 1992; Gallegos and Bevan, 2004). We therefore examined whether negative selection might be affected in the thymus

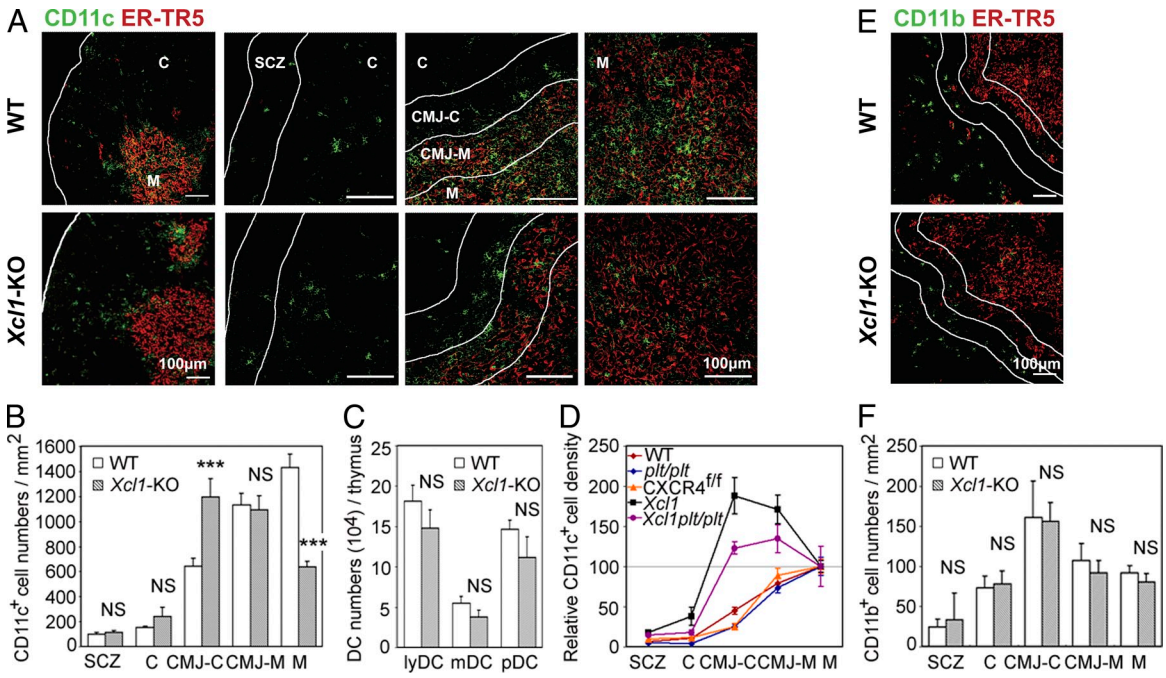

Figure 3. Distribution of DCs and macrophages in the thymus of *Xcl1*-deficient mice. (A) Two-color immunofluorescence analysis of thymus sections stained for CD11c (green) and the mTEC-specific ER-TR5 determinant (red). Representative images from three independent experiments are shown. White lines indicate borders among the indicated regions of the thymus section identified as in Fig. S2 A. C, cortex; M, medulla. Representative images from three independent experiments are shown. (B) Number of CD11c$^+$ cells per unit area (1 mm^2) of the indicated regions of the thymus sections was measured. Means and standard errors of cell numbers from three independent measurements are shown. (C) Means and standard errors (n = 6) of the absolute numbers of lymphoid DCs (lyDCs), myeloid DCs (mDCs), and plasmacytoid DCs (pDCs) in the thymus of indicated mice are shown. (D) Relative density of CD11c$^+$ cells in the indicated regions to the density in the medullary region of the thymus section (in percentile). Means and standard errors (n = 3) for WT, *plt/plt*, Mx-Cre × CXCR4$^{f/f}$, *Xcl1*-deficient, and *Xcl1*-deficient *plt/plt* mice are plotted. (E and F) The thymus sections were analyzed for CD11b (green) and the ER-TR5 determinant (red). Representative images from three independent experiments are shown in E, and means and standard errors of cell numbers from three independent analyses are shown in F. ***, $P < 0.001$. NS, not significant ($P > 0.05$).

of *Xcl1*-deficient mice. As tDCs have been implicated for their roles in negative selection by *mammary tumor virus* (*Mtv*)–encoded superantigens (Moore et al., 1994), we first analyzed the negative selection of Vβ3$^+$, Vβ5$^+$, and Vβ11$^+$ T cells in *Mtv*-expressing BALB/c mice. We found that the deletion of Vβ3$^+$ and Vβ5$^+$ TCR^{high} CD4$^+$CD8$^-$ thymocytes in the *Mtv*$^+$ BALB/c background, as compared with *Mtv*$^-$ C57BL/6 background, was slightly but significantly ($P < 0.05$) disturbed in *Xcl1*-deficient mice (Fig. 4 A). Meanwhile, Vβ3$^+$ and Vβ5$^+$ CD4$^-$CD8$^+$ thymocytes, as well as Vβ11$^+$ thymocytes in CD4$^+$CD8$^-$ and CD4$^-$CD8$^+$ subsets, were deleted comparably in BALB/c mice irrespective of the presence or absence of *Xcl1* (Fig. 4 A). Moreover, the deletion of Vβ3$^+$, Vβ5$^+$, and Vβ11$^+$ T cells detectable in the spleen was not defective in *Xcl1*-deficient BALB/c mice (Fig. S3). Thus, XCL1 plays a minor role in the negative selection of self-*Mtv*–reactive thymocytes.

We then examined whether negative selection of 2C-TCR–transgenic thymocytes reactive to systemically expressed self-antigens (Sha et al., 1988) might be affected by *Xcl1* deficiency. We found that the deletion of 2C-TCR$^+$CD4$^+$CD8$^+$ thymocytes in negatively selecting H-2$^{k/d}$ mice appeared undisturbed in the absence of XCL1 (Fig. 4 B). We further analyzed the role of XCL1 in the negative selection of thymocytes reactive to tissue-restricted antigens that are promiscuously expressed by mTECs. tDCs are known to cooperate with mTECs in the negative selection of thymocytes reactive to tissue-restricted antigens (Gallegos and Bevan, 2004). The rat insulin promoter (RIP)–driven transgene of membrane-bound OVA (mOVA) is expressed in the thymus by mTECs and deletes OVA-reactive OT-I-TCR and OT-II-TCR–transgenic thymocytes (Kurts et al., 1996). We found in irradiation-induced bone marrow chimera experiments that both OT-I-TCR–transgenic CD4$^-$CD8$^+$ and OT-II-TCR–transgenic CD4$^+$CD8$^-$ thymocytes were deleted in the thymic microenvironments of RIP-mOVA–transgenic mice even in the absence of XCL1 (Fig. 4 C), indicating that XCL1 is not needed for the negative selection of thymocytes reactive to the tissue-restricted antigen. These results collectively suggest that the role of XCL1 in negative selection is minor and dispensable.

Defective generation of nT reg cells in *Xcl1*-deficient mice

It was also shown that tDCs play a role in the thymic generation of nT reg cells (Watanabe et al., 2005; Proietto et al., 2008; Hanabuchi et al., 2010). We thus examined whether the generation of nT reg cells in the thymus might be affected in *Xcl1*-deficient mice. We found that CD4$^+$CD8$^-$CD25$^+$Foxp3$^+$

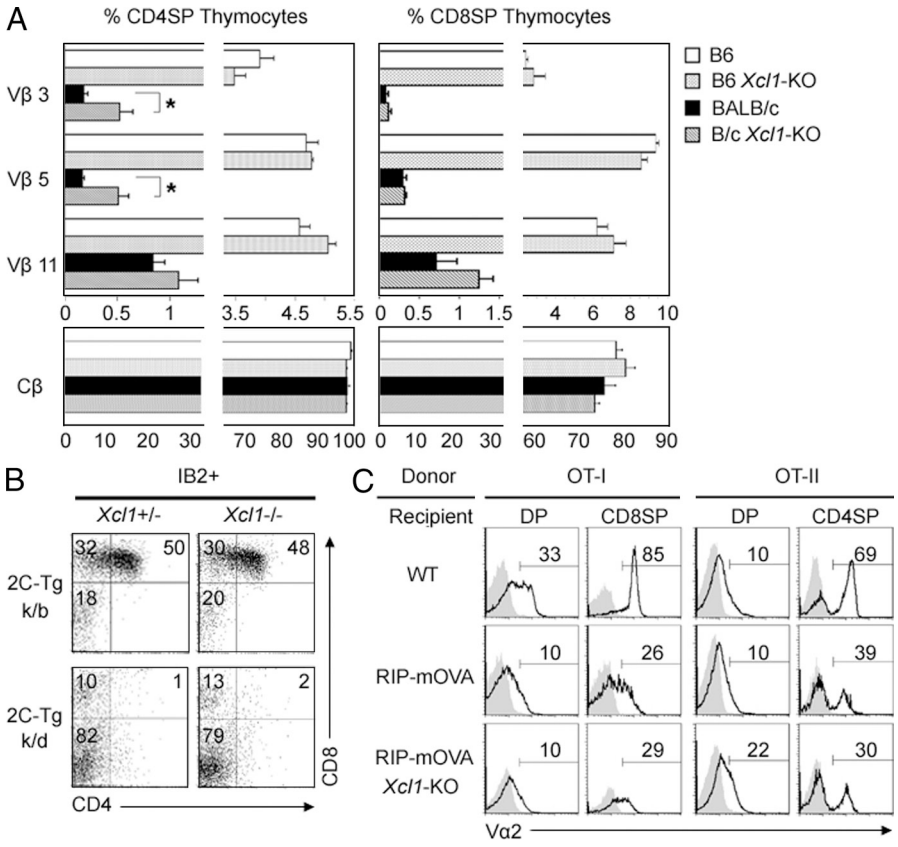

Figure 4. Negative selection of thymocytes in *Xcl1*-deficient mice. (A) Thymocytes isolated from WT and *Xcl1*-deficient (*Xcl1*-KO) mice of C57BL/6 and BALB/c backgrounds were three-color stained for CD4, CD8, and indicated TCR-Vβs. Monoclonal antibodies specific for Cβ, Vβ3, Vβ5, and Vβ11 used were H57-597, KJ25, MR9-4, and KT11, respectively. Shown are the means and standard errors of the frequencies of indicated $V\beta^{high}$ cells within $CD4^+CD8^-$ and $CD4^-CD8^+$ thymocytes from three independent measurements. *, $P < 0.05$. (B) Thymocytes from indicated mouse strains were three-color stained for CD4, CD8, and 2C-TCR (clone 1B2). Shown are the representative profiles of 2C-TCR–expressing cells from three independent experiments. (C) T cell–depleted bone marrow cells from OT-I-TCR–transgenic mice (left) or OT-II-TCR–transgenic mice (right) were transferred into lethally irradiated WT, RIP-mOVA–transgenic (RIP-mOVA), or RIP-mOVA–transgenic *Xcl1*-deficient (RIP-mOVA *Xcl1*-KO) H-2^b mice. Indicated thymocyte populations ($CD4^+CD8^+$, DP; $CD4^+CD8^-$, CD4SP; and $CD4^-CD8^+$, CD8SP) were stained for TCR-Vα2 (solid lines). Shaded profiles represent the analysis with control antibodies. Numbers indicate the frequency of $V\alpha2^{high}$ cells within indicated populations. Representative results of three independent experiments are shown.

T reg cells in the thymus of *Xcl1*-deficient adult mice showed reductions in frequency, as well as in absolute number, when compared with those in the thymus of WT mice (Fig. 5, A and B). The absolute numbers of thymic nT reg cells were significantly ($P < 0.05$) reduced in *Xcl1*-deficient mice throughout ontogeny from the day of birth to 3 mo old (Fig. 5 B). In contrast, the absolute numbers of other populations of thymocytes, including $CD4^-CD8^-$ double-negative, $CD4^+CD8^+$ double-positive, $CD4^+CD8^-$ CD4-single-positive, and $CD4^-CD8^+$ CD8-single-positive thymocytes, were comparable between *Xcl1*-deficient mice and WT mice (Fig. S4 A), indicating that the cell number reduction in the thymus of *Xcl1*-deficient mice was specific for thymic nT reg cells. A majority of $Foxp3^+$ nT reg cells in the thymus were localized in the medullary region (Fontenot et al., 2005; also shown in Fig. 5, C and D). The numbers per unit area of $Foxp3^+$ cells in the middle medullary M region, as well as the peripheral medullary CMJ-M region, were significantly ($P < 0.001$) smaller in *Xcl1*-deficient mice than in WT mice (Fig. 5, C and D). Among $Foxp3^+$ cells in the M and CMJ-M regions, the frequency of $CD11c^+$ DC-attached $Foxp3^+$ cells was severely reduced in *Xcl1*-deficient mice (Fig. 5, E and F), suggesting the role of tDCs in the XCL1-mediated regulation of nT reg cell generation in the thymus. $CD4^+CD8^-CD25^+$ cells isolated from the thymus of *Xcl1*-deficient mice and WT mice comparably suppressed the anti-CD3–stimulated proliferation of $CD4^+CD8^-CD25^-$ conventional T cells (Fig. 5 G), indicating that nT reg cells generated in the thymus of *Xcl1*-deficient mice are functional on a per cell basis but are defective in cell number. These results indicate that XCL1 is needed for the optimal generation of thymic nT reg cells.

Unlike the reduced number of nT reg cells in the thymus, the number of total $Foxp3^+$ cells in the periphery was not reduced in *Xcl1*-deficient mice throughout ontogeny (Fig. S4, B-D). However, the number of thymic nT reg cell–derived spleen nT reg cells, which were identified by the expression of the nuclear factor Helios along with Foxp3 (Sugimoto et al., 2006; Thornton et al., 2010), was reduced in *Xcl1*-deficient mice (Fig. 5 H and Fig. S4 E), suggesting that XCL1 deficiency causes the reduction of nT reg cells in the periphery.

No signs of tissue inflammation were detected in *Xcl1*-deficient mice at 6 wk old and 3 mo old (unpublished data). However, we detected inflammatory lesions and autoantibody deposits in several tissues, including heart, liver, stomach, salivary glands, and lacrimal glands, in *Xcl1*-deficient mice at 12–18 mo old (unpublished data). Importantly, the intravenous transfer of thymocytes from *Xcl1*-deficient BALB/c background mice into athymic BALB/c-*nu/nu* mice caused severe lymphocyte infiltration and tissue damage of lacrimal glands (Fig. 6, A and B). The tissue lesions were prominent in lacrimal glands, weakly detectable in salivary glands, and not detected in heart, liver, stomach, pancreas, or kidney. The administration of equal numbers of WT BALB/c thymocytes along with thymocytes from *Xcl1*-deficient mice significantly reduced the lesions in

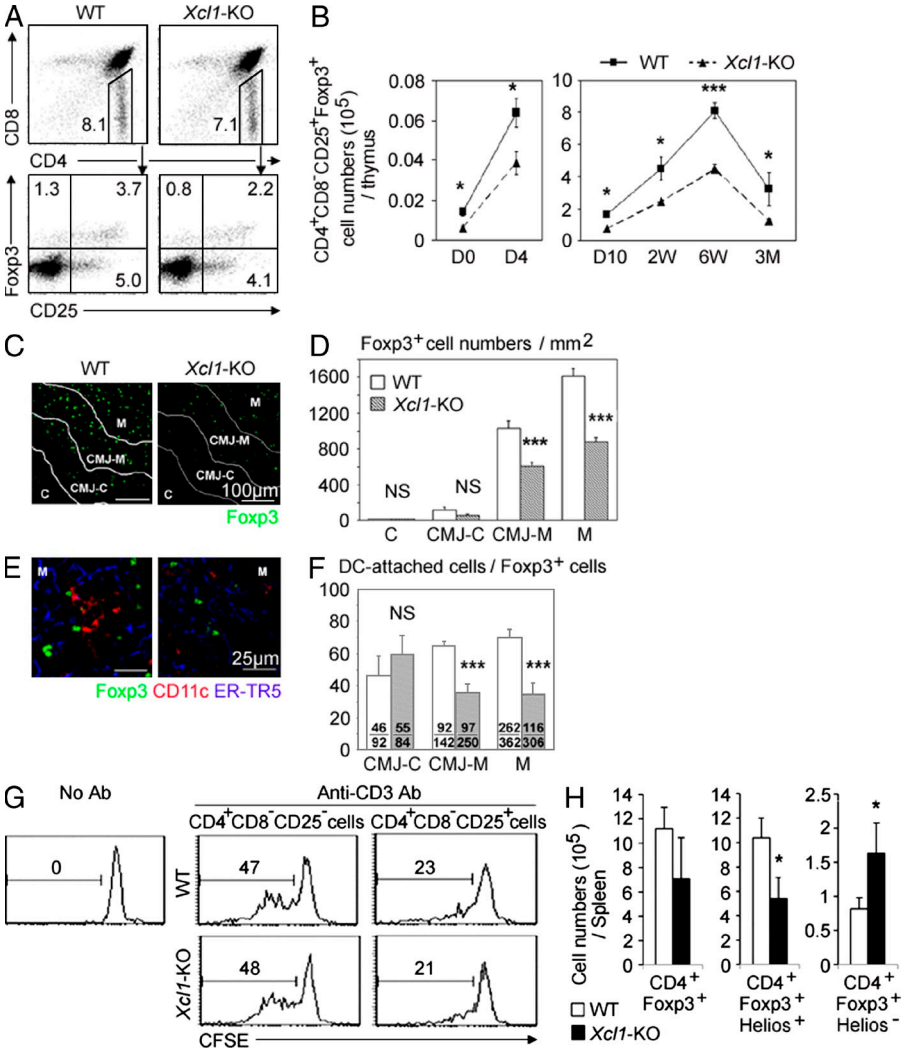

Figure 5. nT reg cell development in *Xcl1*-deficient mice. (A) Thymocytes from indicated mouse strains were four-color stained for CD4, CD8, CD25, and intracellular Foxp3. Numbers indicate the frequency of cells within indicated areas. Shown are the representative results of four independent experiments. (B) Means and standard errors (n = 3–11) of the absolute numbers of $CD4^+CD8^-CD25^+Foxp3^+$ thymocytes in indicated mice at indicated ages. (C) Immunofluorescence analysis of thymus sections from indicated mice for Foxp3. Letters and lines indicate the regions identified as in Fig. S2 A. (D) Numbers of $Foxp3^+$ thymocytes per unit area (1 mm^2) of the indicated regions. Means and standard errors of cell numbers from three independent measurements are shown. (E) Immunofluorescence analysis of thymus sections from indicated mice for Foxp3 (green), CD11c (red), and mTECs (ER-TR5; blue). Magnified images in the M region are shown. (F) Frequency (percentage) of $CD11c^+$ cell–attached cells among $Foxp3^+$ cells in indicated thymic regions. Means and standard errors of the frequencies from eight different images (bars) and the numbers of $CD11c^+$ cell–attached $Foxp3^+$ cells (top) and total $Foxp3^+$ cells (bottom) counted are shown. (G) Representative CFSE fluorescence profiles of $CD4^+CD25^-$ lymph node T cells from B6-Ly5.1 mice cultured in the absence or presence of $CD4^+CD8^-CD25^-$ or $CD4^+CD8^-CD25^+$ thymocytes from WT B6 (top) or *Xcl1*-deficient B6 background mice (bottom) with or without anti-CD3 antibody. Numbers indicate the frequency of $CFSE^{low}$ cells. Representative results of three independent experiments are shown. (H) Intracellular Helios and Foxp3 expression of $CD4^+$ spleen cells from WT and *Xcl1*-KO mice was analyzed by flow cytometry. Shown are the means and standard errors (n = 3) of cell numbers of $Foxp3^+$, $Foxp3^+Helios^+$, and $Foxp3^+Helios^-$ $CD4^+$ spleen cells from WT and *Xcl1*-KO mice. *, $P < 0.05$; ***, $P < 0.001$. NS, not significant ($P > 0.05$).

lacrimal glands (Fig. 6, A and B), suggesting that nT reg cells generated in the normal thymus are capable of suppressing the dacryoadenitis that nT reg cells generated in the thymus of *Xcl1*-deficient mice fail to control. These results indicate that nT reg cell development is impaired in the thymus of *Xcl1*-deficient mice and that the thymocytes from *Xcl1*-deficient mice are potent in causing, and fail to regulate, autoimmune dacryoadenitis.

Aire regulates medullary tDC localization and thymic nT reg cell generation

It was previously shown that $Aire^+$ mTECs play a role in the thymic generation of T reg cells (Aschenbrenner et al., 2007). Finally, we wished to examine whether the expression of Aire might be affected in the thymus of *Xcl1*-deficient mice and whether the expression of XCL1 might be affected in the thymus of *Aire*-deficient mice. The density of $Aire^+$ cells in the thymic medulla was comparable between *Xcl1*-deficient mice and WT mice (Fig. S4, F and G). Quantitative PCR analysis showed that the expression of *Aire* and Aire-dependent tissue-restricted antigens, such as *salivary protein 1*, was not diminished in mTECs isolated from *Xcl1*-deficient mice (unpublished data), indicating that XCL1 is not needed for the expression and function of Aire in mTECs.

In contrast, we found that the expression of *Xcl1* transcripts was severely defective in mTECs that were isolated from *Aire*-deficient mice (Fig. 7 A). As has been recently reported (Laan et al., 2009), the expression of other chemokines, such as *Ccl19*, *Ccl21*, and *Ccl25*, in mTECs was also modulated by the *Aire* deficiency (Fig. 7 A). However, the reduction of *Xcl1* in *Aire*-deficient mTECs was remarkably severe (the expression of which reduced to ∼1% of that observed in normal mTECs), which is in contrast to the relatively mild alterations in the expression of the other chemokines in *Aire*-deficient mTECs (15–200% of the amount in normal mTECs; Fig. 7 A).

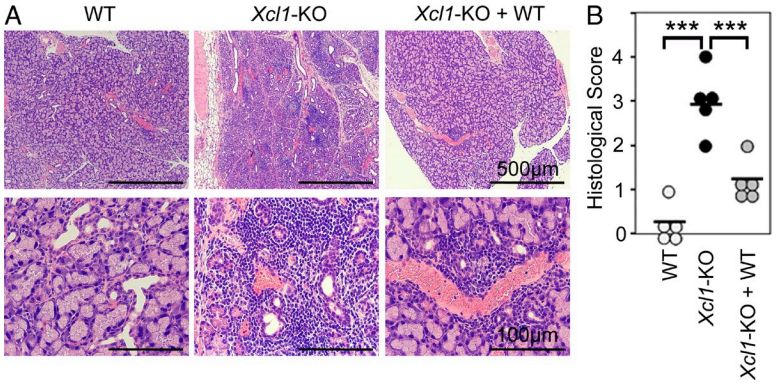

Figure 6. Thymocytes from *Xcl1*-deficient mice elicit inflammatory lesions in lacrimal glands in *nude* mice. 5×10^7 thymocytes isolated from WT or *Xcl1*-deficient (*Xcl1*-KO) mice of BALB/c background were intravenously transferred into BALB/c-*nu*/*nu* mice. Where indicated, equal numbers of thymocytes ($5 \times 10^7 + 5 \times 10^7$) were mixed before the transfer. Paraffin-embedded sections of lacrimal glands at 8 wk after the transfer were stained with hematoxylin and eosin. (A) Representative images of the sections at two different magnifications. (B) Histological scores of inflammatory lesions in the lacrimal glands ($n = 5$). Horizontal bars indicate the means. ***, $P < 0.001$.

The density of tDCs in the middle medullary M region was significantly ($P < 0.01$) decreased in *Aire*-deficient mice, whereas that in the CMJ-C region was significantly ($P < 0.05$) elevated in *Aire*-deficient mice (Fig. 7, B and C). The density of tDCs in the other regions (SCZ, C, and CMJ-M regions) was not significantly ($P > 0.05$) altered by the *Aire* deficiency (Fig. 7, B and C). The absolute numbers of tDCs and their subsets were not affected in *Aire*-deficient mice (Fig. 7 D). These results indicate that as in *Xcl1*-deficient mice, *Aire*-deficient mice exhibit defective accumulation of tDCs in the medullary region.

The density of Foxp3$^+$ cells in the thymic medulla (CMJ-M and M regions) was accordingly and significantly ($P < 0.05$) lower in *Aire*-deficient mice than in WT mice (Fig. 7, E and F). Moreover, the absolute number of CD4$^+$CD8$^-$CD25$^+$Foxp3$^+$ cells in the thymus was significantly ($P < 0.05$) reduced in *Aire*-deficient mice (Fig. 7 G). These results indicate that *Aire*-deficient mice exhibit defective generation of nT reg cells in the thymus.

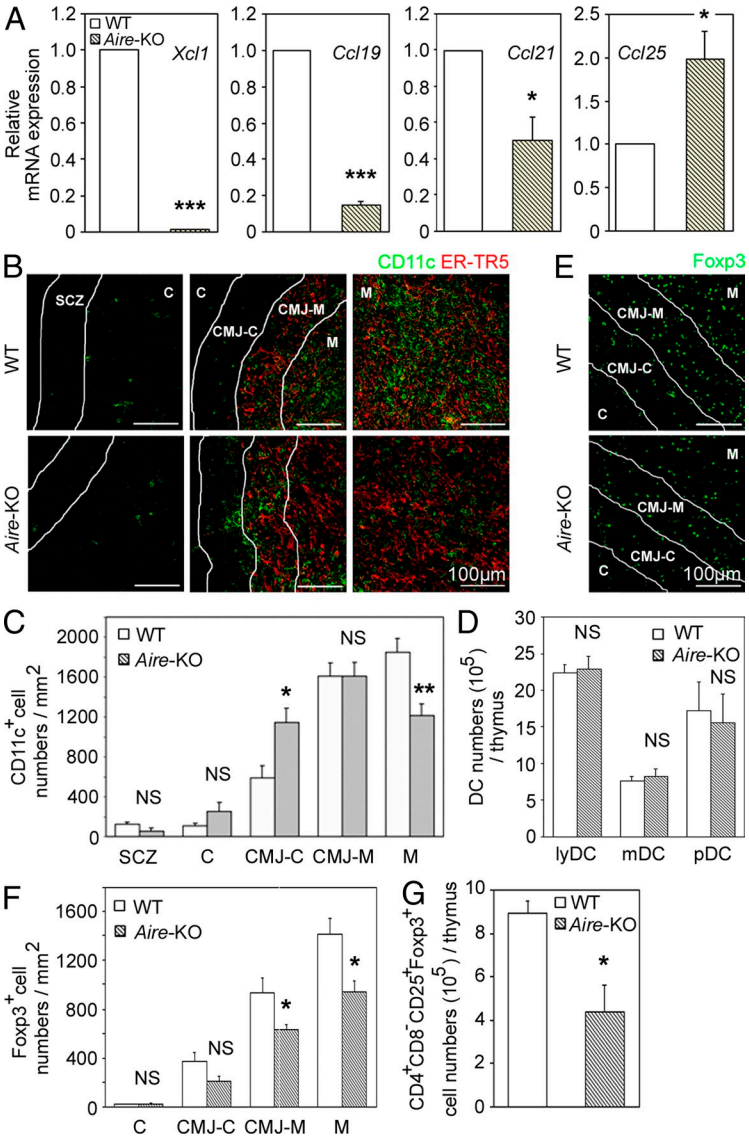

Figure 7. DCs and T reg cells in the thymus of *Aire*-deficient mice. (A) Quantitative RT-PCR analysis of *Xcl1*, *Ccl19*, *Ccl21*, and *Ccl25* expression in sorted CD45$^-$EpCAM$^+$UEA1$^+$ mTECs from WT and *Aire*-deficient mice. The amounts of the transcripts were normalized to the amount of housekeeping *Hprt*, and those in WT mTECs were arbitrarily set to 1. Bar graphs show means and standard errors of at least three independent measurements. (B) Immunofluorescence analysis of thymus sections for CD11c (green) and mTECs (ER-TR5; red). Representative images from two independent experiments are shown. Lines indicate borders among the indicated regions identified as in Fig. S2 A. (C) Numbers of CD11c$^+$ cells per unit area (1 mm^2) of the indicated regions were measured. Means and standard errors of cell numbers are shown. (D) Means and standard errors ($n = 3$–4) of the absolute numbers of indicated DC subpopulations in the thymus of indicated mouse strains are shown. (E) Immunofluorescence analysis of thymus sections from indicated mice for Foxp3. Representative images from two independent experiments are shown. (F) Numbers of Foxp3$^+$ cells per unit area (1 mm^2) of the indicated areas were measured. Means and standard errors of cell numbers from three independent measurements are shown. (G) Means and standard errors ($n = 3$) of the absolute numbers of CD4$^+$CD8$^-$CD25$^+$Foxp3$^+$ cells in the thymus of indicated mice. *, $P < 0.05$; **, $P < 0.01$; ***, $P < 0.001$. NS, not significant ($P > 0.05$).

DISCUSSION

It is well known that tDCs are detected abundantly in the medullary region and sparsely in the cortical region (Barclay and Mayrhofer, 1981; Flotte et al., 1983; Kurobe et al., 2006). However, the molecular mechanisms that contribute to this medullary accumulation of tDCs are unknown. Screening for the chemokine receptors expressed by tDCs and their chemotactic responses to candidate ligands has revealed that the chemokine ligands for CCR7, CXCR4, and XCR1 are capable of attracting tDCs. By analyzing mice deficient for these chemokine ligands or their receptors, we identify that the XCL1–XCR1 chemokine axis plays a potent role in the medullary accumulation of tDCs. In contrast, we find that CCR7 and CXCR4 play a minor, if any, role in the accumulation of tDCs in the thymic medulla.

XCL1, which is also known as lymphotactin, ATAC, and SCM1, is the only member of the C family of chemokines encoded in the mouse genome (Kelner et al., 1994). XCL1 is produced by activated $CD8^+$ T cells, Th1-polarized $CD4^+$ T cells, and NK cells (Kelner et al., 1994; Hedrick et al., 1997; Dorner et al., 2002, 2004, 2009). A recent study shows that the XCL1 receptor, XCR1, is expressed by $CD8^+$ DCs in the spleen and that the XCL1-XCR1–mediated interaction between $CD8^+$ T cells and $CD8^+$ DCs is important for the development of cytotoxicity of $CD8^+$ T cells to antigens cross-presented by $CD8^+$ DCs (Dorner et al., 2009). However, the functions of the XCL1–XCR1 chemokine axis in the thymus have remained unknown. This study reveals the role of the XCL1–XCR1 chemokine axis in the localization of tDCs in the thymic medulla.

In the thymus, XCR1 is exclusively expressed by tDCs. Among the tDC subpopulations, XCR1 is most highly detectable in I-$A^{high}$$CD11c^{high}$$CD11b^-$ lymphoid DCs, a population that largely overlaps with the $CD8^+Sirp\alpha^-$ conventional DC subpopulation of tDCs (Wu and Shortman, 2005). In contrast, XCL1 in the thymus is expressed in the class II MHC^{high} subpopulation of mTECs in addition to NK and NKT cells. The *Xcl1* transcripts expressed by mTECs are in smaller amounts than those expressed by activated $CD8^+$ T cells in the spleen but are prominent in the thymus when compared with those expressed by other cells in the thymus, including cTECs, thymic fibroblasts, tDCs, or $CD45^+$ thymocytes. In *Xcl1*-deficient mice, tDCs fail to localize in the medullary region and are instead accumulated in the deep cortex and CMJ regions, although the numbers and subpopulations of tDCs are not altered. The mislocalization of tDCs in the deep cortex and CMJ regions of the thymus was detected in irradiated *Xcl1*-deficient mice that were reconstituted with normal bone marrow cells but not in irradiated normal mice that were reconstituted with *Xcl1*-deficient bone marrow cells (unpublished data). These results suggest that XCL1 produced by irradiation-resistant thymic stromal cells, rather than irradiation-sensitive bone marrow–derived thymocytes, contributes to the attraction of XCR1-expressing tDCs into the inner medullary region of the thymus. We think that mTECs, rather than hematopoietic cells including NK cells and NKT cells, in the thymus play a major role in the XCL1-mediated medullary localization of tDCs.

The arrest of tDCs in the deep cortex and CMJ regions in *Xcl1*-deficient mice suggests that the tDCs that are accumulated in the medullary region of normal mice may be derived from tDCs that are either generated in the deep cortex and CMJ regions of the thymus or migrate into the thymus from the circulation at the deep cortex and CMJ regions. The XCL1-mediated attraction of XCR1-expressing tDCs to the medulla may facilitate efficient interactions between mTECs and tDCs. It is also possible that the distribution of tDCs may be further regulated by the balance between the XCL1-mediated attraction to the medullary region and the attraction to the deep cortex and CMJ regions by unknown factors, and the loss of XCL1 may result in the aberrant attraction of tDCs to the deep cortex and CMJ regions.

Our results also reveal that Aire is essential for the production of XCL1 by mTECs. Aire is a nuclear factor expressed by a subpopulation of mTECs and is implicated for its role in the promiscuous gene expression of tissue-restricted self-antigens in mTECs (Derbinski et al., 2005; Mathis and Benoist, 2009). It is also suggested that Aire regulates the development of mTECs, thereby indirectly contributing to the promiscuous gene expression in mTECs (Gillard et al., 2007; Yano et al., 2008). Our results show that the expression of *Xcl1* transcripts in mTECs isolated from *Aire*-deficient mice is severely reduced to ~1% of the amount observed in WT mTECs. Accordingly, as in *Xcl1*-deficient mice, the medullary accumulation of tDCs is severely impaired in *Aire*-deficient mice and the tDCs are aberrantly arrested in the deep cortex and CMJ regions. Aire may regulate the development of XCL1-producing mTECs. Alternatively, Aire may promiscuously regulate the expression of *Xcl1* gene in mTECs.

Concomitant with the failure in the medullary accumulation of tDCs, mice deficient for either *Xcl1* or *Aire* exhibit a reduction in the number of T reg cells generated in the thymus. Most T reg cells in the thymus are generated in the medullary region (Fontenot et al., 2005) and it is suggested that mTECs (Aschenbrenner et al., 2007; Spence and Green, 2008), tDCs (Proietto et al., 2008; Hanabuchi et al., 2010), and their cooperation (Watanabe et al., 2005) contribute to the generation of T reg cells in the thymus. Our results indicate that the deficiency of either *Xcl1* or *Aire* causes the reduced generation of T reg cells in the thymus. The cellularity of thymic T reg cells in *Xcl1*-deficient mice and *Aire*-deficient mice is approximately half of that in WT mice and is significantly low when compared with that in WT mice. However, the reduced numbers of thymic T reg cells are not significantly ($P > 0.05$) different between *Xcl1*-deficient mice and *Aire*-deficient mice. Our results also indicate that *Aire* deficiency causes severe loss of XCL1 expression by mTECs, whereas *Xcl1* deficiency does not reduce Aire expression by mTECs. We therefore think that Aire is essential for the mTEC expression of XCL1, which attracts XCR1-expressing tDCs to the medullary region and contributes to the optimal generation of T reg cells in the thymus.

Proximal interactions between tDCs and mTECs in the thymic medulla may promote optimal generation of nT reg cells, possibly via the production of γc cytokines, including IL-2, IL-7, and thymic stromal lymphopoietin (Watanabe et al., 2005; Ziegler and Liu, 2006; Mazzucchelli et al., 2008; Vang et al., 2008). Among the tDC subpopulations, lymphoid DCs most highly express XCR1 and, thus, may play a major role in the interaction with mTECs and the generation of nT reg cells. Unlike tDCs, $CD4^+CD8^-CD25^+$ thymic T reg cells do not express detectable *Xcr1* transcripts (unpublished data), ruling out the possibility of a direct effect of XCL1 on T reg cells. Thus, our results suggest that XCL1-producing mTECs attract tDCs into the inner medullary region, thereby promoting the generation of nT reg cells, and that optimal nT reg cell development in the thymus requires a specialized medullary microenvironment that is formed by the XCL1-mediated attraction of tDCs by Aire-dependent mTECs. Whether XCL1-mediated tDC accumulation in the medulla affects TCR repertoire of nT reg cells remains unclear.

A recent work using CD11c-Cre mice crossed with mice that express diphtheria toxin A under the control of a loxP-flanked neomycin resistance cassette from the ROSA26 locus has shown that these DC-depleted mice are not defective in the generation of nT reg cells in the thymus (Ohnmacht et al., 2009), potentially contradicting our results indicating the role of tDCs in nT reg cell generation. However, that work also described that the depletion of tDCs is incomplete in the DC-depleted mice (Ohnmacht et al., 2009) but did not describe the intrathymic localization of the remaining tDCs. Thus, the incompletely depleted tDCs in the DC-depleted mice may be enriched in the inner medullary region and be sufficient for the unreduced generation of nT reg cells.

Our results show that the number of nT reg cells in the thymus is reduced in *Aire*-deficient mice. However, several studies have described that the generation of T reg cells is not defective in *Aire*-deficient mice (Anderson et al., 2002, 2005; Liston et al., 2003; Kuroda et al., 2005; Hubert et al., 2009), particularly in the spleen and the lymph nodes (Anderson et al., 2005; Kuroda et al., 2005; Hubert et al., 2009). Indeed, our results show that the number of T reg cells in *Aire*-deficient mice is reduced in the thymus to approximately half of that in WT mice but is not reduced in the spleen and the lymph nodes of *Aire*-deficient mice. It should be noted that previous studies have indicated that the number of T reg cells in the thymus is slightly reduced in *Aire*-deficient mice, although those studies concluded no loss of T reg cell generation in the thymus (Anderson et al., 2005; Kuroda et al., 2005; Hubert et al., 2009). We think that Aire indeed contributes to the optimal generation of nT reg cells in the thymus and that the generation of induced T reg cells, particularly in the periphery (Piccirillo and Shevach, 2004; Curotto de Lafaille and Lafaille, 2009), has veiled the reduced cellularity of nT reg cells in *Aire*-deficient mice.

The present results show that thymocytes from *Xcl1*-deficient mice are potent in eliciting severe lymphocyte infiltration and tissue damage of lacrimal glands in athymic *nu/nu* mice, indicating that the thymocytes generated in *Xcl1*-deficient mice fail to establish self-tolerance. The mixture of thymocytes from normal mice reduces the dacryoadenitis caused by the thymocytes from *Xcl1*-deficient mice, supporting the possibility that the thymocytes from *Xcl1*-deficient mice are potent in triggering, and fail to regulate, the autoimmunity and that nT reg cell development is impaired in the thymus of *Xcl1*-deficient mice. In a similar manner, *Aire*-deficient mice tend to exhibit inflammatory failure of exocrine tissues, including lacrimal glands (Anderson et al., 2002, 2005; Kuroda et al., 2005; Hubert et al., 2009). The commonness of the target organs may reflect a similarity in the breakdown of self-tolerance in *Xcl1*-deficient mice and *Aire*-deficient mice. Nonetheless, our results do not rule out the possibility that the absence of XCL1 in peripheral T cells also contributes to the onset of the dacryoadenitis.

Finally, our results reveal that the XCL1-mediated medullary accumulation of tDCs plays only a minor role in the negative selection of self-reactive thymocytes. In contrast, tDCs are known for their roles in negative selection, particularly in the intrathymic presentation of peripheral antigens, by cooperating with promiscuous gene expression in mTECs (Gallegos and Bevan, 2004; Koble and Kyewski, 2009; Nitta et al., 2009) and by transport from the circulation (Bonasio et al., 2006). The tDCs that are mislocalized in the CMJ regions in the absence of XCL1 may be sufficient for the cross-presentation of mTEC-expressed tissue-restricted antigens and the negative selection of developing thymocytes reactive to those self-antigens. In addition, recent studies indicated that DCs in the thymic cortex are capable of inducing the deletion of negatively selected thymocytes (McCaughtry et al., 2008) and that CCR2 is involved in the accumulation of $CD8^-Sirp\alpha^+$ tDC subpopulation in the thymic cortex and the intrathymic negative selection against blood-borne antigens (Baba et al., 2009). Thus, the XCL1-mediated medullary accumulation is not needed for the deletion of the majority of negatively selected thymocytes.

In conclusion, the present results indicate that the XCL1–XCR1 chemokine axis contributes to the medullary accumulation of tDCs and the thymic development of nT reg cells. The results also suggest that Aire expressed in mTECs regulates the XCL1-mediated medullary accumulation of tDCs and that XCL1-mediated proximal interaction between tDCs and mTECs in the thymic medulla contributes to the thymic development of nT reg cells. Our results imply a novel role of Aire in regulating autoimmunity via the XCL1-mediated medullary accumulation of tDCs and that the breakdown of self-tolerance in Aire deficiency may involve the failure to localize tDCs in the medulla in an XCL1-dependent manner.

MATERIALS AND METHODS

Mice. *Xcl1*-deficient mice were generated at Merck Research Laboratories (Fig. S1, A–C). *Aire*-deficient mice were generated at the University of Basel (Fig. S5). *Ccr7*-deficient mice (Förster et al., 1999), Mx-Cre x $Cxcr4^{flox/flox}$ mice (Sugiyama et al., 2006), and *plt/plt* mice (Nakano et al., 1998), as well as OT-I and OT-II TCR-transgenic and RIP-mOVA–transgenic mice (Kurts et al., 1996; Barnden et al., 1998), were described previously. Mx-Cre x $Cxcr4^{flox/flox}$ mice were injected with poly I poly C, and only mice that

exhibited a nearly complete loss of CXCR4 genomic sequence and the undetectable expression of CXCR4 gene in hematopoietic cells were further analyzed (Sugiyama et al., 2006). Mice were maintained under specific pathogen-free conditions in our animal facility, and experiments were performed under the approval of the Institutional Animal Care Committee of the University of Tokushima.

Bone marrow chimeras. Bone marrow cells were magnetically depleted of T cells using biotin-conjugated antibodies specific for CD4, CD8, and Thy1.2 and streptavidin-conjugated magnetic beads (Miltenyi Biotec). Recipient mice were injected with T cell–depleted bone marrow cells (4×10^7) 1 d after 9.25 Gy x-ray irradiation. The mice were analyzed 4–5 wk after the reconstitution.

Thymocyte transfer into *nude* mice. 5×10^7 thymocytes isolated from WT or *Xcl1*-deficient (*Xcl1*-KO) mice of BALB/c background were intravenously transferred into BALB/c-*nu/nu* mice. Where indicated, equal numbers of thymocytes ($5 \times 10^7 + 5 \times 10^7$) were mixed before the transfer. Various organs at 8 wk after the transfer were fixed with 4% phosphate-buffered formaldehyde, pH 7.2. Paraffin-embedded sections were stained with hematoxylin and eosin. Two pathologists independently evaluated the histology without being informed of the conditions of individual mice. Inflammatory lesions of the tissues were scored as previously described (Ishimaru et al., 2008) and as follows: 0 = no inflammation, 1 = 1–5 foci composed of >20 mononuclear cells per focus, 2 = >5 such foci but without significant parenchymal destruction, 3 = degeneration of parenchymal tissue, and 4 = extensive infiltration with mononuclear cells and extensive parenchymal destruction.

Flow cytometry analysis. Multicolor flow cytometry analysis and cell sorting were performed using FACSCalibur and FACSAria II (BD). Intracellular staining of Foxp3 and Helios was performed according to the manufacturer's instructions (eBioscience). Thymic stromal cells were prepared by digesting thymic fragments with collagenase, dispase, and DNase I (Roche) and enriched by depleting $CD45^+$ cells with a magnetic cell sorter (Miltenyi Biotec) before cell sorting, as described previously (Gray et al., 2002). For DC analysis, thymus cells were prepared by digesting thymic fragments with collagenase D and DNase I.

Immunofluorescence analysis. Frozen thymus tissues embedded in OCT compound (Sakura) were sliced into 5-µm-thick sections, fixed with acetone, and stained with the following antibodies: mTEC-specific monoclonal antibody ER-TR5 (a gift from W. van Ewijk, Erasmus University, Rotterdam, Netherlands) followed by Alexa Fluor 633–conjugated anti–rat IgG antibody (Invitrogen); biotinylated UEA1 (Vector Laboratories) followed by Alexa Fluor 633–conjugated streptavidin (Invitrogen); FITC-conjugated anti-Foxp3 monoclonal antibody (eBioscience); biotinylated anti-CD11c or anti-CD11b monoclonal antibody (eBioscience) followed by Alexa Fluor 488–conjugated or Alexa Fluor 546–conjugated streptavidin (Invitrogen); and anti-Aire antibody (Santa Cruz Biotechnology, Inc.) followed by FITC-conjugated anti–rabbit IgG antibody (Invitrogen). Images were analyzed with a TSC SP2 confocal laser-scanning microscope and Confocal software version 2.6 (Leica).

Chemotaxis assay. 10^6 collagenase-digested thymus cells were placed in a Transwell chamber (6.5-mm diameter, 5-µm pore; Corning) that was inserted into a 100-nM chemokine-containing culture well. Cells were incubated for 2 h, counted, stained for CD11c and $I\text{-}A^b$, and analyzed by flow cytometry. Chemotactic index is the ratio of the numbers of $CD11c^+I\text{-}A^{b+}$ DCs that migrated to the bottom of culture wells in the presence and absence of chemokines.

Measurement of T reg cell function. According to the methods previously reported (Tai et al., 2005), 5×10^4 CFSE-labeled $CD4^+CD25^-$ lymph node T cells isolated from B6-Ly5.1 mice were cultured with 5×10^4 $CD25^+CD4^+CD8^-$ or $CD25^-CD4^+CD8^-$ thymocytes in the presence of 10^5 20 Gy-irradiated T cell–depleted spleen cells from B6 mice and 1 µg/ml anti-CD3 monoclonal antibody (clone 2C11). Cells were harvested at 72 h and analyzed by flow cytometry.

RT-PCR analysis. Total cellular RNA was reverse transcribed with oligo-dT primer and Superscript III reverse transcription (Invitrogen). cDNA was PCR amplified, electrophoresed, and visualized with ethidium bromide. For quantitative analysis, real-time RT-PCR was performed using SYBR Premix Ex Taq (Takara Bio Inc.) and Light Cycler DX400 (Roche). Amplified products were confirmed to be single bands by gel electrophoresis and were normalized to the amount of HPRT products. Primer sequences are listed in Table S1.

Statistical analysis. Statistical comparison was performed with the Student's *t* test (two-tailed) using Excel software (Microsoft).

Online supplemental material. Fig. S1 shows genomic structure of *Xcl1*-deficient mice. Fig. S2 shows analysis of $CD11c^+$ cells in thymus sections. Fig. S3 shows negative selection of T cells in the periphery of *Xcl1*-deficient mice. Fig. S4 shows thymocytes, splenocytes, and $Aire^+$ mTECs in *Xcl1*-deficient mice. Fig. S5 shows targeting strategy to generate *Aire*-Cre-GFP knockin mice. Table S1 shows primer sequences used for RT-PCR analysis. Online supplemental material is available at http://www.jem.org/cgi/content/full/jem.20102327/DC1.

We would like to express our special appreciation to the late professor Cunlan Liu for initiating the present study. We also would like to thank Tomoo Ueno and Fumi Saito for technical support in the laboratory and Kensuke Takada for reading the manuscript.

This study was supported by a MEXT Grant-in-Aid for Scientific Research on Priority Area "Immunological Self", the JST Strategic International Cooperative Program, the Swiss National Science Foundation, the European Framework Programme 6, and the Max Planck Society.

The authors have no competing financial interests.

Submitted: 5 November 2010
Accepted: 12 January 2011

REFERENCES

Anderson, G., P.J. Lane, and E.J. Jenkinson. 2007. Generating intrathymic microenvironments to establish T-cell tolerance. *Nat. Rev. Immunol.* 7:954–963. doi:10.1038/nri2187

Anderson, M.S., E.S. Venanzi, L. Klein, Z. Chen, S.P. Berzins, S.J. Turley, H. von Boehmer, R. Bronson, A. Dierich, C. Benoist, and D. Mathis. 2002. Projection of an immunological self shadow within the thymus by the Aire protein. *Science.* 298:1395–1401. doi:10.1126/science.1075958

Anderson, M.S., E.S. Venanzi, Z. Chen, S.P. Berzins, C. Benoist, and D. Mathis. 2005. The cellular mechanism of Aire control of T cell tolerance. *Immunity.* 23:227–239. doi:10.1016/j.immuni.2005.07.005

Aschenbrenner, K., L.M. D'Cruz, E.H. Vollmann, M. Hinterberger, J. Emmerich, L.K. Swee, A. Rolink, and L. Klein. 2007. Selection of $Foxp3^+$ regulatory T cells specific for self antigen expressed and presented by $Aire^+$ medullary thymic epithelial cells. *Nat. Immunol.* 8:351–358. doi:10.1038/ni1444

Baba, T., Y. Nakamoto, and N. Mukaida. 2009. Crucial contribution of thymic Sirp α^+ conventional dendritic cells to central tolerance against bloodborne antigens in a CCR2-dependent manner. *J. Immunol.* 183:3053–3063. doi:10.4049/jimmunol.0900438

Barclay, A.N., and G. Mayrhofer. 1981. Bone marrow origin of Ia-positive cells in the medulla rat thymus. *J. Exp. Med.* 153:1666–1671. doi:10.1084/jem.153.6.1666

Barnden, M.J., J. Allison, W.R. Heath, and F.R. Carbone. 1998. Defective TCR expression in transgenic mice constructed using cDNA-based alpha- and beta-chain genes under the control of heterologous regulatory elements. *Immunol. Cell Biol.* 76:34–40. doi:10.1046/j.1440-1711.1998.00709.x

Bonasio, R., M.L. Scimone, P. Schaerli, N. Grabie, A.H. Lichtman, and U.H. von Andrian. 2006. Clonal deletion of thymocytes by circulating

dendritic cells homing to the thymus. *Nat. Immunol.* 7:1092–1100. doi:10.1038/ni1385

Curotto de Lafaille, M.A., and J.J. Lafaille. 2009. Natural and adaptive foxp3$^+$ regulatory T cells: more of the same or a division of labor? *Immunity.* 30:626–635. doi:10.1016/j.immuni.2009.05.002

Derbinski, J., A. Schulte, B. Kyewski, and L. Klein. 2001. Promiscuous gene expression in medullary thymic epithelial cells mirrors the peripheral self. *Nat. Immunol.* 2:1032–1039. doi:10.1038/ni723

Derbinski, J., J. Gäbler, B. Brors, S. Tierling, S. Jonnakuty, M. Hergenhahn, L. Peltonen, J. Walter, and B. Kyewski. 2005. Promiscuous gene expression in thymic epithelial cells is regulated at multiple levels. *J. Exp. Med.* 202:33–45. doi:10.1084/jem.20050471

Dorner, B.G., A. Scheffold, M.S. Rolph, M.B. Huser, S.H. Kaufmann, A. Radbruch, I.E. Flesch, and R.A. Kroczek. 2002. MIP-1α, MIP-1β, RANTES, and ATAC/lymphotactin function together with IFN-γ as type 1 cytokines. *Proc. Natl. Acad. Sci. USA.* 99:6181–6186. doi:10.1073/pnas.092141999

Dorner, B.G., H.R. Smith, A.R. French, S. Kim, J. Poursine-Laurent, D.L. Beckman, J.T. Pingel, R.A. Kroczek, and W.M. Yokoyama. 2004. Coordinate expression of cytokines and chemokines by NK cells during murine cytomegalovirus infection. *J. Immunol.* 172:3119–3131.

Dorner, B.G., M.B. Dorner, X. Zhou, C. Opitz, A. Mora, S. Güttler, A. Hutloff, H.W. Mages, K. Ranke, M. Schaefer, et al. 2009. Selective expression of the chemokine receptor XCR1 on cross-presenting dendritic cells determines cooperation with CD8$^+$ T cells. *Immunity.* 31:823–833. doi:10.1016/j.immuni.2009.08.027

Flotte, T.J., T.A. Springer, and G.J. Thorbecke. 1983. Dendritic cell and macrophage staining by monoclonal antibodies in tissue sections and epidermal sheets. *Am. J. Pathol.* 111:112–124.

Fontenot, J.D., J.P. Rasmussen, L.M. Williams, J.L. Dooley, A.G. Farr, and A.Y. Rudensky. 2005. Regulatory T cell lineage specification by the forkhead transcription factor foxp3. *Immunity.* 22:329–341. doi:10.1016/j.immuni.2005.01.016

Förster, R., A. Schubel, D. Breitfeld, E. Kremmer, I. Renner-Müller, E. Wolf, and M. Lipp. 1999. CCR7 coordinates the primary immune response by establishing functional microenvironments in secondary lymphoid organs. *Cell.* 99:23–33. doi:10.1016/S0092-8674(00)80059-8

Gallegos, A.M., and M.J. Bevan. 2004. Central tolerance to tissue-specific antigens mediated by direct and indirect antigen presentation. *J. Exp. Med.* 200:1039–1049. doi:10.1084/jem.20041457

Gillard, G.O., J. Dooley, M. Erickson, L. Peltonen, and A.G. Farr. 2007. Aire-dependent alterations in medullary thymic epithelium indicate a role for Aire in thymic epithelial differentiation. *J. Immunol.* 178:3007–3015.

Gray, D.H., A.P. Chidgey, and R.L. Boyd. 2002. Analysis of thymic stromal cell populations using flow cytometry. *J. Immunol. Methods.* 260:15–28. doi:10.1016/S0022-1759(01)00493-8

Hanabuchi, S., T. Ito, W.R. Park, N. Watanabe, J.L. Shaw, E. Roman, K. Arima, Y.H. Wang, K.S. Voo, W. Cao, and Y.J. Liu. 2010. Thymic stromal lymphopoietin-activated plasmacytoid dendritic cells induce the generation of FOXP3$^+$ regulatory T cells in human thymus. *J. Immunol.* 184: 2999–3007. doi:10.4049/jimmunol.0804106

Hedrick, J.A., V. Saylor, D. Figueroa, L. Mizoue, Y. Xu, S. Menon, J. Abrams, T. Handel, and A. Zlotnik. 1997. Lymphotactin is produced by NK cells and attracts both NK cells and T cells in vivo. *J. Immunol.* 158: 1533–1540.

Hubert, F.X., S.A. Kinkel, P.E. Crewther, P.Z. Cannon, K.E. Webster, M. Link, R. Uibo, M.K. O'Bryan, A. Meager, S.P. Forehan, et al. 2009. Aire-deficient C57BL/6 mice mimicking the common human 13-base pair deletion mutation present with only a mild autoimmune phenotype. *J. Immunol.* 182:3902–3918. doi:10.4049/jimmunol.0802124

Ishimaru, N., R. Arakaki, S. Yoshida, A. Yamada, S. Noji, and Y. Hayashi. 2008. Expression of the retinoblastoma protein RbAp48 in exocrine glands leads to Sjögren's syndrome-like autoimmune exocrinopathy. *J. Exp. Med.* 205:2915–2927. doi:10.1084/jem.20080174

Jenkinson, E.J., G. Anderson, and J.J. Owen. 1992. Studies on T cell maturation on defined thymic stromal cell populations in vitro. *J. Exp. Med.* 176:845–853. doi:10.1084/jem.176.3.845

Kelner, G.S., J. Kennedy, K.B. Bacon, S. Kleyensteuber, D.A. Largaespada, N.A. Jenkins, N.G. Copeland, J.F. Bazan, K.W. Moore, T.J. Schall, and A. Zlotnik. 1994. Lymphotactin: a cytokine that represents a new class of chemokine. *Science.* 266:1395–1399. doi:10.1126/science.7973732

Klein, L., M. Hinterberger, G. Wirnsberger, and B. Kyewski. 2009. Antigen presentation in the thymus for positive selection and central tolerance induction. *Nat. Rev. Immunol.* 9:833–844. doi:10.1038/nri2669

Koble, C., and B. Kyewski. 2009. The thymic medulla: a unique microenvironment for intercellular self-antigen transfer. *J. Exp. Med.* 206:1505–1513. doi:10.1084/jem.20082449

Kurobe, H., C. Liu, T. Ueno, F. Saito, I. Ohigashi, N. Seach, R. Arakaki, Y. Hayashi, T. Kitagawa, M. Lipp, et al. 2006. CCR7-dependent cortex-to-medulla migration of positively selected thymocytes is essential for establishing central tolerance. *Immunity.* 24:165–177. doi:10.1016/j.immuni.2005.12.011

Kuroda, N., T. Mitani, N. Takeda, N. Ishimaru, R. Arakaki, Y. Hayashi, Y. Bando, K. Izumi, T. Takahashi, T. Nomura, et al. 2005. Development of autoimmunity against transcriptionally unrepressed target antigen in the thymus of Aire-deficient mice. *J. Immunol.* 174:1862–1870.

Kurts, C., W.R. Heath, F.R. Carbone, J. Allison, J.F. Miller, and H. Kosaka. 1996. Constitutive class I–restricted exogenous presentation of self antigens in vivo. *J. Exp. Med.* 184:923–930. doi:10.1084/jem.184.3.923

Laan, M., K. Kisand, V. Kont, K. Möll, L. Tserel, H.S. Scott, and P. Peterson. 2009. Autoimmune regulator deficiency results in decreased expression of CCR4 and CCR7 ligands and in delayed migration of CD4$^+$ thymocytes. *J. Immunol.* 183:7682–7691. doi:10.4049/jimmunol.0804133

Liston, A., S. Lesage, J. Wilson, L. Peltonen, and C.C. Goodnow. 2003. Aire regulates negative selection of organ-specific T cells. *Nat. Immunol.* 4:350–354. doi:10.1038/ni906

Mathis, D., and C. Benoist. 2009. Aire. *Annu. Rev. Immunol.* 27:287–312. doi:10.1146/annurev.immunol.25.022106.141532

Mazzucchelli, R., J.A. Hixon, R. Spolski, X. Chen, W.Q. Li, V.L. Hall, J. Willette-Brown, A.A. Hurwitz, W.J. Leonard, and S.K. Durum. 2008. Development of regulatory T cells requires IL-7Ralpha stimulation by IL-7 or TSLP. *Blood.* 112:3283–3292. doi:10.1182/blood-2008-02-137414

McCaughtry, T.M., T.A. Baldwin, M.S. Wilken, and K.A. Hogquist. 2008. Clonal deletion of thymocytes can occur in the cortex with no involvement of the medulla. *J. Exp. Med.* 205:2575–2584. doi:10.1084/jem.20080866

Moore, N.C., G. Anderson, D.E. McLoughlin, J.J. Owen, and E.J. Jenkinson. 1994. Differential expression of Mtv loci in MHC class II-positive thymic stromal cells. *J. Immunol.* 152:4826–4831.

Nakano, H., S. Mori, H. Yonekawa, H. Nariuchi, A. Matsuzawa, and T. Kakiuchi. 1998. A novel mutant gene involved in T-lymphocyte-specific homing into peripheral lymphoid organs on mouse chromosome 4. *Blood.* 91:2886–2895.

Nitta, T., S. Nitta, Y. Lei, M. Lipp, and Y. Takahama. 2009. CCR7-mediated migration of developing thymocytes to the medulla is essential for negative selection to tissue-restricted antigens. *Proc. Natl. Acad. Sci. USA.* 106:17129–17133. doi:10.1073/pnas.0906956106

Ohnmacht, C., A. Pullner, S.B. King, I. Drexler, S. Meier, T. Brocker, and D. Voehringer. 2009. Constitutive ablation of dendritic cells breaks self-tolerance of CD4 T cells and results in spontaneous fatal autoimmunity. *J. Exp. Med.* 206:549–559. doi:10.1084/jem.20082394

Piccirillo, C.A., and E.M. Shevach. 2004. Naturally-occurring CD4$^+$CD25$^+$ immunoregulatory T cells: central players in the arena of peripheral tolerance. *Semin. Immunol.* 16:81–88. doi:10.1016/j.smim.2003.12.003

Proietto, A.I., S. van Dommelen, P. Zhou, A. Rizzitelli, A. D'Amico, R.J. Steptoe, S.H. Naik, M.H. Lahoud, Y. Liu, P. Zheng, et al. 2008. Dendritic cells in the thymus contribute to T-regulatory cell induction. *Proc. Natl. Acad. Sci. USA.* 105:19869–19874. doi:10.1073/pnas.0810268105

Sakaguchi, S., T. Yamaguchi, T. Nomura, and M. Ono. 2008. Regulatory T cells and immune tolerance. *Cell.* 133:775–787. doi:10.1016/j.cell.2008.05.009

Sha, W.C., C.A. Nelson, R.D. Newberry, D.M. Kranz, J.H. Russell, and D.Y. Loh. 1988. Positive and negative selection of an antigen receptor on T cells in transgenic mice. *Nature.* 336:73–76. doi:10.1038/336073a0

Spence, P.J., and E.A. Green. 2008. Foxp3$^+$ regulatory T cells promiscuously accept thymic signals critical for their development. *Proc. Natl. Acad. Sci. USA.* 105:973–978. doi:10.1073/pnas.0709071105

Sugimoto, N., T. Oida, K. Hirota, K. Nakamura, T. Nomura, T. Uchiyama, and S. Sakaguchi. 2006. Foxp3-dependent and -independent molecules specific

for CD25$^+$CD4$^+$ natural regulatory T cells revealed by DNA microarray analysis. *Int. Immunol.* 18:1197–1209. doi:10.1093/intimm/dxl060

Sugiyama, T., H. Kohara, M. Noda, and T. Nagasawa. 2006. Maintenance of the hematopoietic stem cell pool by CXCL12-CXCR4 chemokine signaling in bone marrow stromal cell niches. *Immunity.* 25:977–988. doi:10.1016/j.immuni.2006.10.016

Tai, X., M. Cowan, L. Feigenbaum, and A. Singer. 2005. CD28 costimulation of developing thymocytes induces Foxp3 expression and regulatory T cell differentiation independently of interleukin 2. *Nat. Immunol.* 6:152–162. doi:10.1038/ni1160

Takahama, Y. 2006. Journey through the thymus: stromal guides for T-cell development and selection. *Nat. Rev. Immunol.* 6:127–135. doi:10.1038/nri1781

Thornton, A.M., P.E. Korty, D.Q. Tran, E.A. Wohlfert, P.E. Murray, Y. Belkaid, and E.M. Shevach. 2010. Expression of Helios, an Ikaros transcription factor family member, differentiates thymic-derived from peripherally induced Foxp3$^+$ T regulatory cells. *J. Immunol.* 184:3433–3441. doi:10.4049/jimmunol.0904028

Vang, K.B., J. Yang, S.A. Mahmud, M.A. Burchill, A.L. Vegoe, and M.A. Farrar. 2008. IL-2, -7, and -15, but not thymic stromal lymphopoietin, redundantly govern CD4$^+$Foxp3$^+$ regulatory T cell development. *J. Immunol.* 181:3285–3290.

Watanabe, N., Y.H. Wang, H.K. Lee, T. Ito, Y.H. Wang, W. Cao, and Y.J. Liu. 2005. Hassall's corpuscles instruct dendritic cells to induce CD4$^+$CD25$^+$ regulatory T cells in human thymus. *Nature.* 436:1181–1185. doi:10.1038/nature03886

Wu, L., and K. Shortman. 2005. Heterogeneity of thymic dendritic cells. *Semin. Immunol.* 17:304–312. doi:10.1016/j.smim.2005.05.001

Yano, M., N. Kuroda, H. Han, M. Meguro-Horike, Y. Nishikawa, H. Kiyonari, K. Maemura, Y. Yanagawa, K. Obata, S. Takahashi, et al. 2008. Aire controls the differentiation program of thymic epithelial cells in the medulla for the establishment of self-tolerance. *J. Exp. Med.* 205:2827–2838. doi:10.1084/jem.20080046

Ziegler, S.F., and Y.J. Liu. 2006. Thymic stromal lymphopoietin in normal and pathogenic T cell development and function. *Nat. Immunol.* 7:709–714. doi:10.1038/ni1360